Chapter 3 Hydrogen plasma passivation of GaAs solar cells grown on Si substrate

3. 1 Introduction

GaAs grown on Si substrate (GaAs/Si) is a very promising material for realizing high efficiency, low cost, and light weight solar cells[1]. However, high density of dislocations (~10^6 -10^7 cm^{-2}) exist in the GaAs/Si due to the large lattice mismatch (~ 4.1%) and large thermal expansion coefficient mismatch (~ 60%) between GaAs and Si, which seriously degrades the photovoltaic properties of GaAs/Si solar cells. Both the short-circuit current and the open-circuit voltage of GaAs/Si solar cell are reduced dramatically by the presence of dislocation-associated non radiative recombination centers which reduces the minority carrier lifetime[2]. To improve the conversion efficiency of the GaAs/Si solar cells, several attempts have been made, such as using the thermal cycle annealing (TCA) procedure[3], inducing suitable buffer layer[4] and graded band-gap emitter layer (GBEL)[5], and utilizing the back surface field (BSF) structure[6]. As a result, the total efficiency of the GaAs/Si monolithic 3-terminal tandem solar cell of 19.9% has been obtained under the AM0 measurement condition (1 sun, 135.3 mW/cm^2, 27°C)[7]. However, for further improving the efficiency of the GaAs/Si solar cells for practical application, it needs to reduce the dislocation density in GaAs/Si as low as 10^4 cm^{-2}. Since the reduction of the density of threading dislocations to such a low level in GaAs/Si epilayers can't be simply realized, passivation of the electrical activities of these defects is becoming very essential. Passivation of a wide range of shallow and deep impurities in GaAs by hydrogen (H_2) plasma exposure has been intensively investigated[8, 9]. As describted in chapter 2, it is found that incorporation of H atoms in GaAs/Si helps to reduce the density of electrically active dangling bonds and passivate the electrical activity of most defects and impurity states[10], and the beneficial effects of the H plasma passivation are stable under usual device processing temperature (below 450°C)[11]. However, exposure to H plasma induces surface roughness and depletion of As

from the GaAs surface[12], and, sometimes, the damage effects exceed the H passivation effects. It needs to recover these damages without removing the beneficial passivation effects of the H atoms incorporation.

In this chapter, we present a detailed study of H_2 plasma exposure and annealing effects on the photovoltaic properties of GaAs solar cells grown on Si substrates. It is found that the conversion efficiency of the H_2 plasma passivated GaAs/Si solar cell is improved, and this improvement is stable under the 450°C annealing in AsH_3 ambient, which is the usual solar cell process temperature. This can be attributed to the increased minority carrier lifetime by the H passivation of the defect-related non radiative recombination centers in GaAs/Si. The organization of this chapter is as follows: In section 3. 2, the growth of GaAs solar cells on Si substrates used in the present experiment are described. The H_2 plasma passivation and annealing effects on photovoltaic properties of GaAs solar cells grown on Si substrates are characterized in chapter 3. 3. Finally, this chapter is summarized in section 3. 4.

3. 2 Experiment Procedure

The p^+-n GaAs single-junction solar cells were made on (100) 2° off towards [011] Si substrate by using a conventional atmospheric pressure metalorganic chemical vapor deposition (MOCVD). Trimethylgallium (TMG), trimethylalluminum (TMA) and AsH_3 were used as the source materials for Ga, Al and As, respectively. Diethylzinc (DEZ) and H_2Se were used as the p-type and n-type doping source materials , respectively. The two-step growth technique was used. After the growth of a 1.5 μm thick GaAs buffer layer at 750°C, the thermal cycle annealing (TCA) from 300°C to 900°C was carried out 5 times to improve the quality of the GaAs film on Si. Then the p^+-n GaAs single junction solar cells were grown at 750°C followed by the growth of 50-nm p^+-$Al_{0.8}Ga_{0.2}As$ window layer at 800°C. The detailed solar cell structure is shown in Fig. 3. 1. After the growth process, the epilayers were transferred into the plasma reactor, as described in chapter 2, through

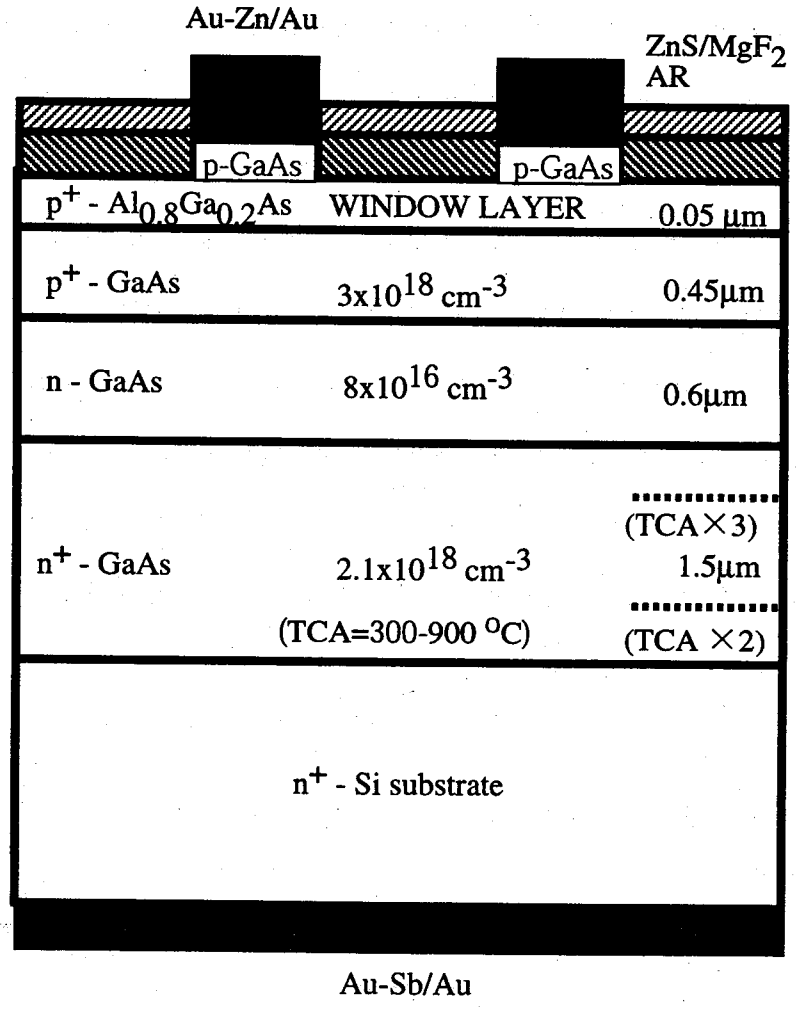

Fig. 3. 1 The schematic cross-sectional structure of GaAs single-junction solar cell grown on Si substrate by MOCVD.

which H_2 is pumped at a reduced pressure (~0.1 Torr) to complete the H_2 plasma passivation. The plasma input power was changed from 60 to 120 W. The GaAs/Si sample is heated up to 250°C at 0.1 Torr downstream from the plasma. Post-passivation annealing were also performed at different temperatures for 10 minutes in AsH_3/H_2 (AsH_3/H_2=10%) ambient. Then AuZn/Au and AuSb/Au were formed as the electrodes for the p^+-GaAs layer and n^+-Si substrate, respectively. Anti reflection coatings (ARC) were made of MgF_2/ZnS double layers. The total area of the GaAs solar cell is 5×5 mm^2. Time-resolved photoluminescence is excited by the semiconductor laser pulse (λ=655 nm, duration=50ps) and the time-resolved photoluminescence (TRP) decay curves are measured at room temperature using the photon counting method for an AlGaAs (50 nm)/GaAs (1μm) double hetero-structure grown on Si substrate. The photovoltaic properties of these cells were measured under AM0, 1 sun conditions at 27°C using a solar simulator. The values of photovoltaic properties discussed are active-area values.

3. 3 Charactrization of hydrogen plasma passivaton effect on GaAs solar cell on Si

3. 3. 1 Study of minority carrier lifetime

For optoelectronic devices, e.g. lasers or solar cells, the minority carrier recombination plays a major role in determining device performance. Neglecting the AlGaAs/GaAs interface recombination, the lifetime of minority carrier can be calculated by the slope of the decay curve. Figure 3. 2 shows the minority carrier (hole) lifetime of the samples obtained from the TRP decay curves, which are taken before and after hydrogen plasma exposure, and after post-passivation annealing at different temperatures. The lifetime is found to increase from 1.66 to 2.66 ns after the H plasma passivation. This increase can be attributed to the passivation effects of shallow and deep levels in GaAs/Si by H incorporation. After annealing the passivated samples at 450°C to restore the majority carrier concentration, a increased lifetime (2.27 ns) is still remained. It means that the

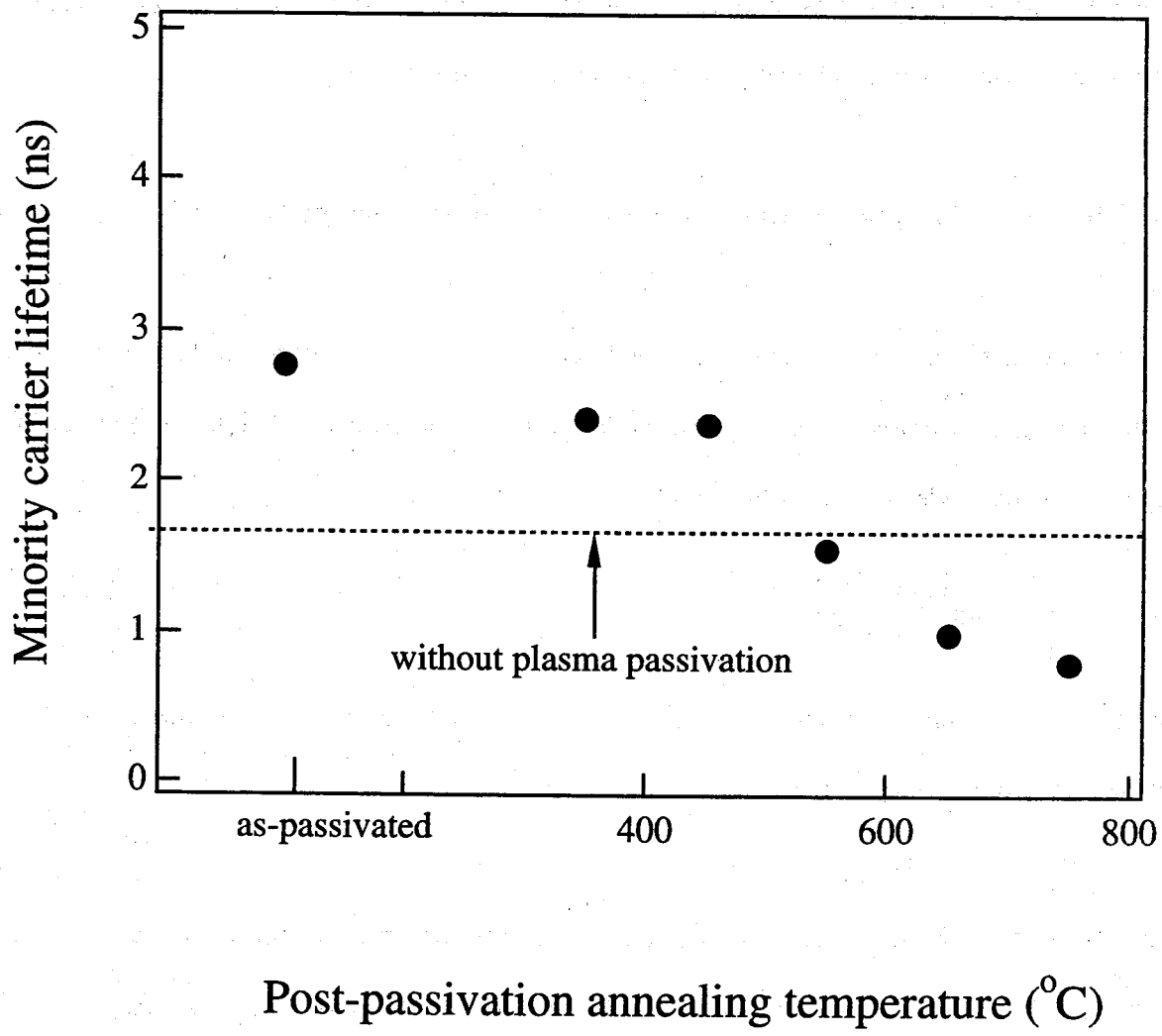

Fig. 3. 2 Minority carrier lifetimes obtained from non intentionally doped n-AlGaAs/GaAs (1 μm) DH structure on Si before and after H_2 plasma passivation, and after annealed in AsH_3 ambient for different temperatures, respectively. The H_2 plasma passivation conditions are: 250°C, 0.1 Torr, 1h.

passivation effects of some deep defects in GaAs/Si is stable under 450°C annealing[13], as described in chapter 2. When the annealing temperature exceeds 650°C, the H passivation effects are completely removed and the plasma-induced damages is activated simultaneously. As a result, the lifetime is decreased, even compared with that of as-grown sample.

3. 3. 2 Study of the photovoltaic properties of GaAs solar cells on Si

In a p-n junction solar cell structure, the total curent in the diode connect to the external load is given by the light generated curent and the diode current in the absence of light. In general, if the voltage across the diode is V, the total curent is

$$I = I_L + I_0\left[1 - \exp\left\{\frac{e(V + R_s I)}{mk_B T}\right\}\right] \tag{3.1}$$

where I_L is the photocurrent, I_0 is the reverse saturation current, R_s is the diode series resistance, m is the ideality factor.

$$I_L = I_{nL} + I_{pL} + I_L = eG_L(L_p + L_n + W)A \tag{3.2}$$

where G_L is the *e-h generation rate,* L_p and L_n are the diffusion length of hole and electron, respectively, W is the width of depletion region. A is the area of the salr cell.

To calculate the important parameters of solar cell, consider the case where the diode is used in the open circuit mode so that the crrent I is zero. Thus gives

$$I = 0 = I_L - I_0\left[\exp\left(\frac{eV_{oc}}{mk_B T}\right) - 1\right] \tag{3.3}$$

where V_{oc} is the voltage across the diode and is known as the open circuit voltage. We get for this voltage

$$V_{oc} = \frac{mk_B T}{e}\ln\left(1 + \frac{I_L}{I_o}\right) \tag{3.4}$$

A second limiting case in the solar cell is the one where the output is short circuited, i.e., R=0 and V=0. The short circuit current is then

$$I = I_{sc} = I_L \tag{3.5}$$

The conversion efficiency of a solar cell is defined as the rate of the output electrical power to the input optical power. When the solar cell is operating under maximum power conditions at a voltage and current value of V_m and I_m, the conversion efficiency is

$$E_{ff} = \frac{P_m}{P_{in}} \times 100\% = \frac{I_m V_m}{P_{in}} \times 100\% \tag{3.6}$$

Another useful parameter in defining solar cell parameters is the fill factor FF, defined as

$$FF = \frac{I_m V_m}{I_{sc} V_{oc}} \tag{3.7}$$

From above description, it is clearly seen that to improve the short circuit current I_{sc}, it needs to increase the minority carrier lifetime, and hence increase the minority carrier diffusion length L_p and L_n. For a given I_L, the open circuit voltage increases logarithmicaly with decreasing saturation current I_0.

Figure 3. 3 shows the photovoltaic properties of H_2 plasma passivated GaAs/Si solar cells as a function of post-passivation annealing temperature in AsH_3/H_2 ambient. Here, the H_2 plasma passivation was performed at 250°C, 0.1 Torr, 90 W for 1h. Compared with that of the cell before H_2 plasma passivation (16.6%), an efficient increase in short circuit current density (J_{sc}) and open circuit voltage (V_{oc}) were realized due to the passivation of nonradiative recombination centers in GaAs/Si solar cell, as a result, a highest conversion efficiencies of 18.3% was obtained only by H_2 plasma exposure. The increase in J_{sc} is mainly attributed to the increase in the minority carrier lifetime, as shown in Fig. 3.2. The increase in V_{oc} is mainly attributed to the decrease in the I_0, as observed in the dark I-V characteristics. After annealing the passivated cell at 450 °C for 10 min in AsH_3 ambient, a conversion efficiencies of 17.2% still remained with a restored carrier concentration. We also annealed the H_2 plasma passivated cell in pure H_2 ambient at 450°C, but the

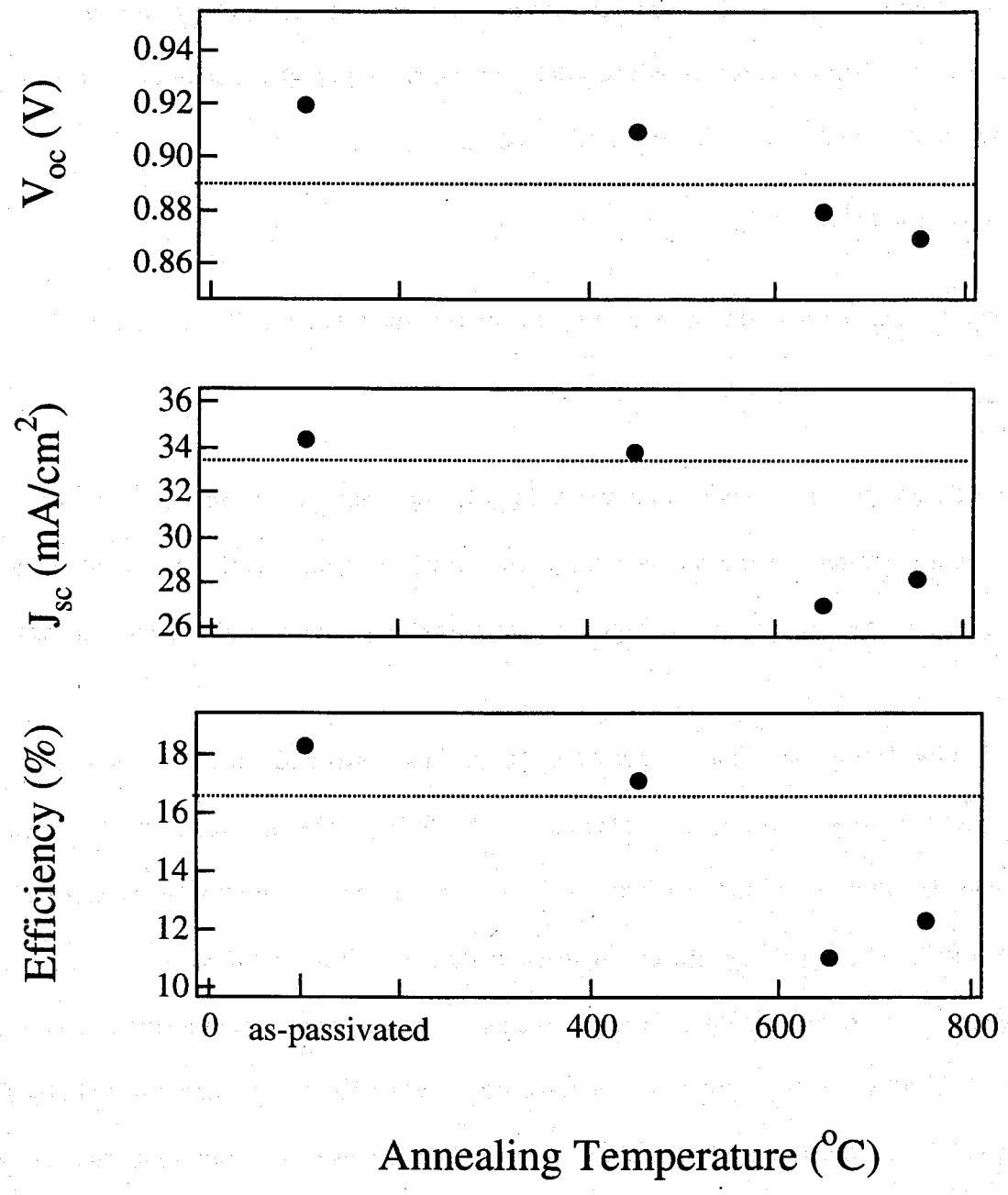

Fig. 3. 3 The photovoltaic properties of GaAs/Si solar cells before and after H_2 plasma passivation, and as a function of post-passivation annealing temperatures in AsH_3/H_2 ambient, respectively. The H_2 plasma passivation conditions are: 250 ^oC, 0.1 Torr, 90 W, 1h.

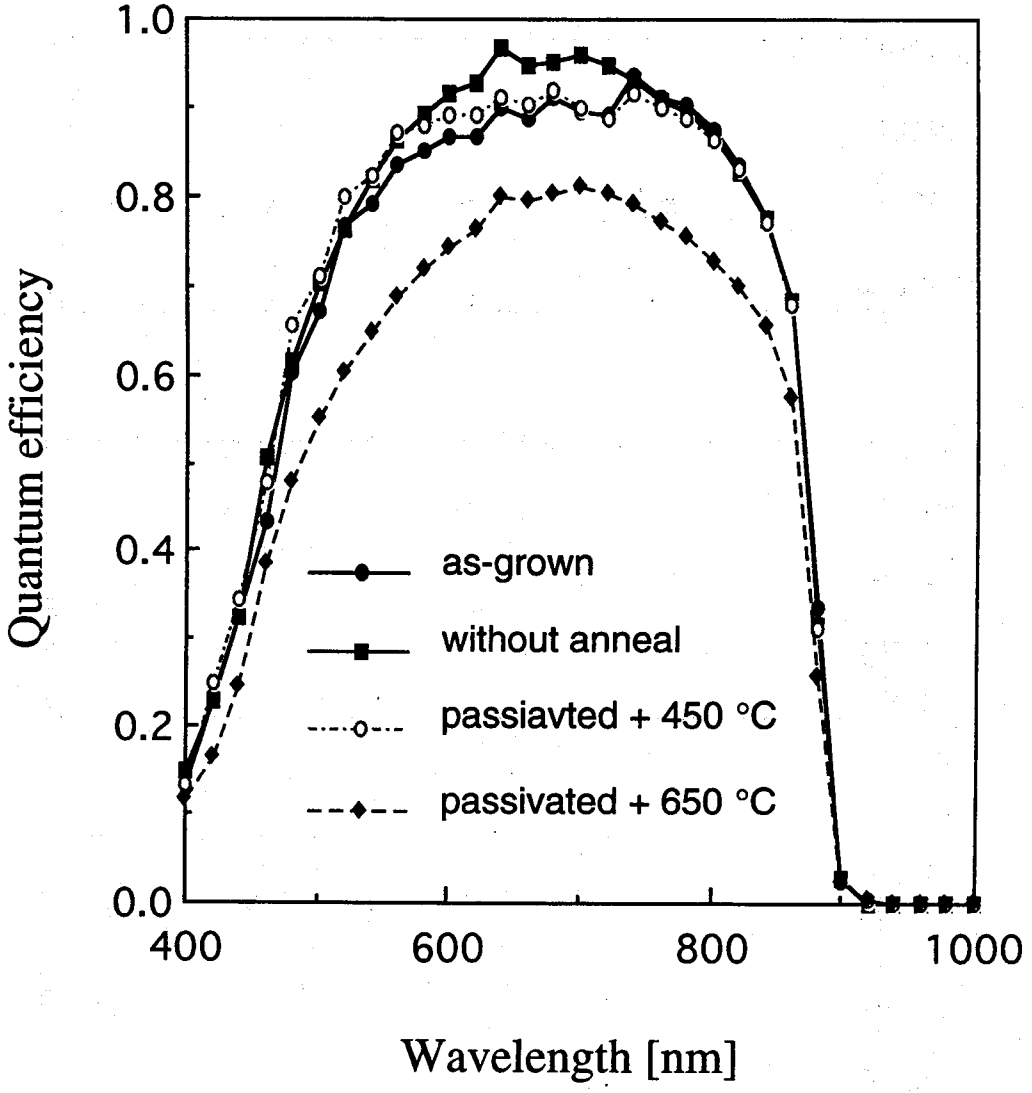

Fig. 3. 4 Quantum efficiencies of GaAs solar cells on Si substrates with various plasma treatment conditions.

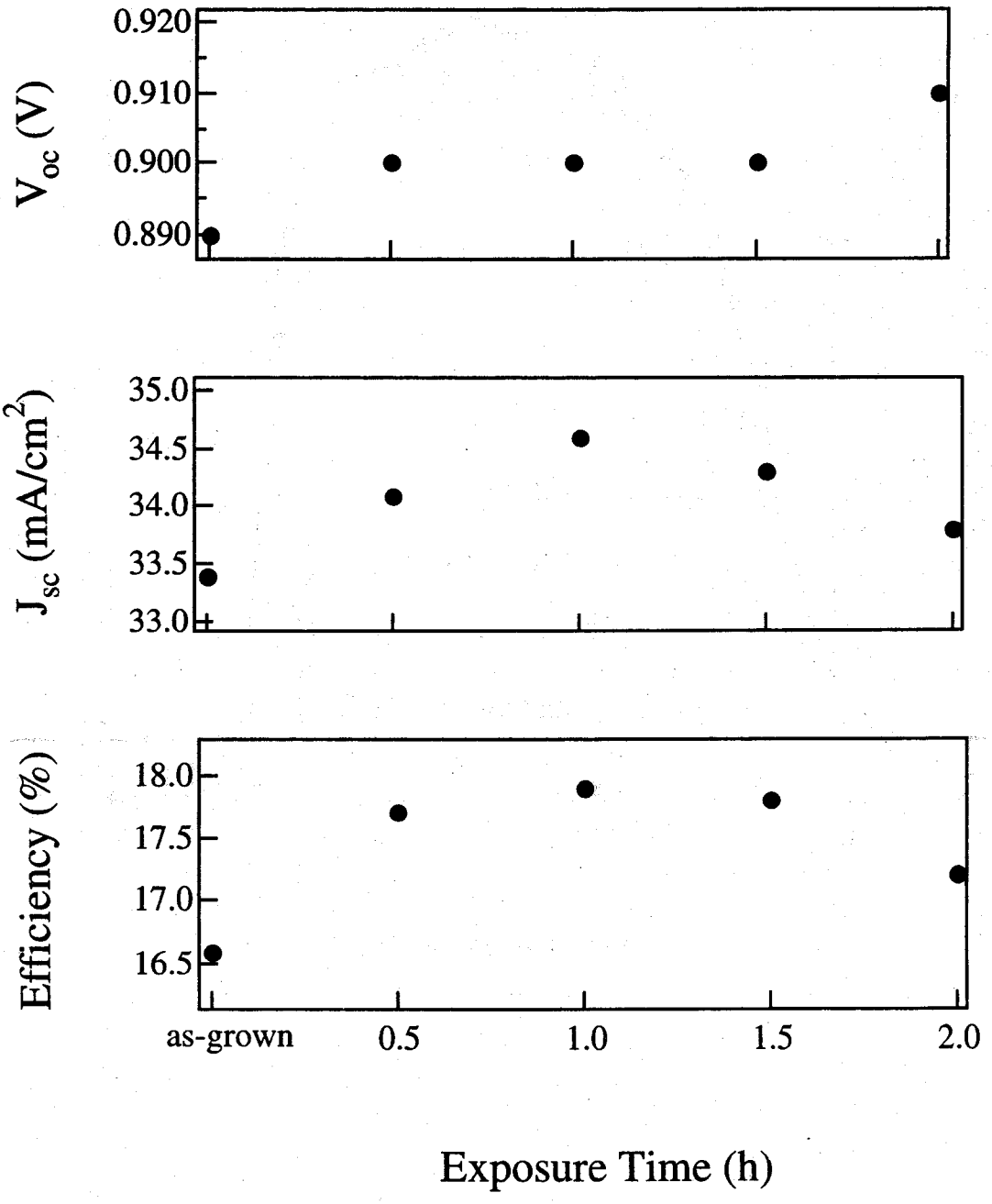

Fig. 3. 5 The photovoltaic properties of GaAs/Si solar cells as a function of H_2 plasma exposure time. The plasma input power is 90 W, and the temperature is 250°C. The post-passivation annealing conditions were fixed at 450°C for 10 min in AsH_3 ambient.

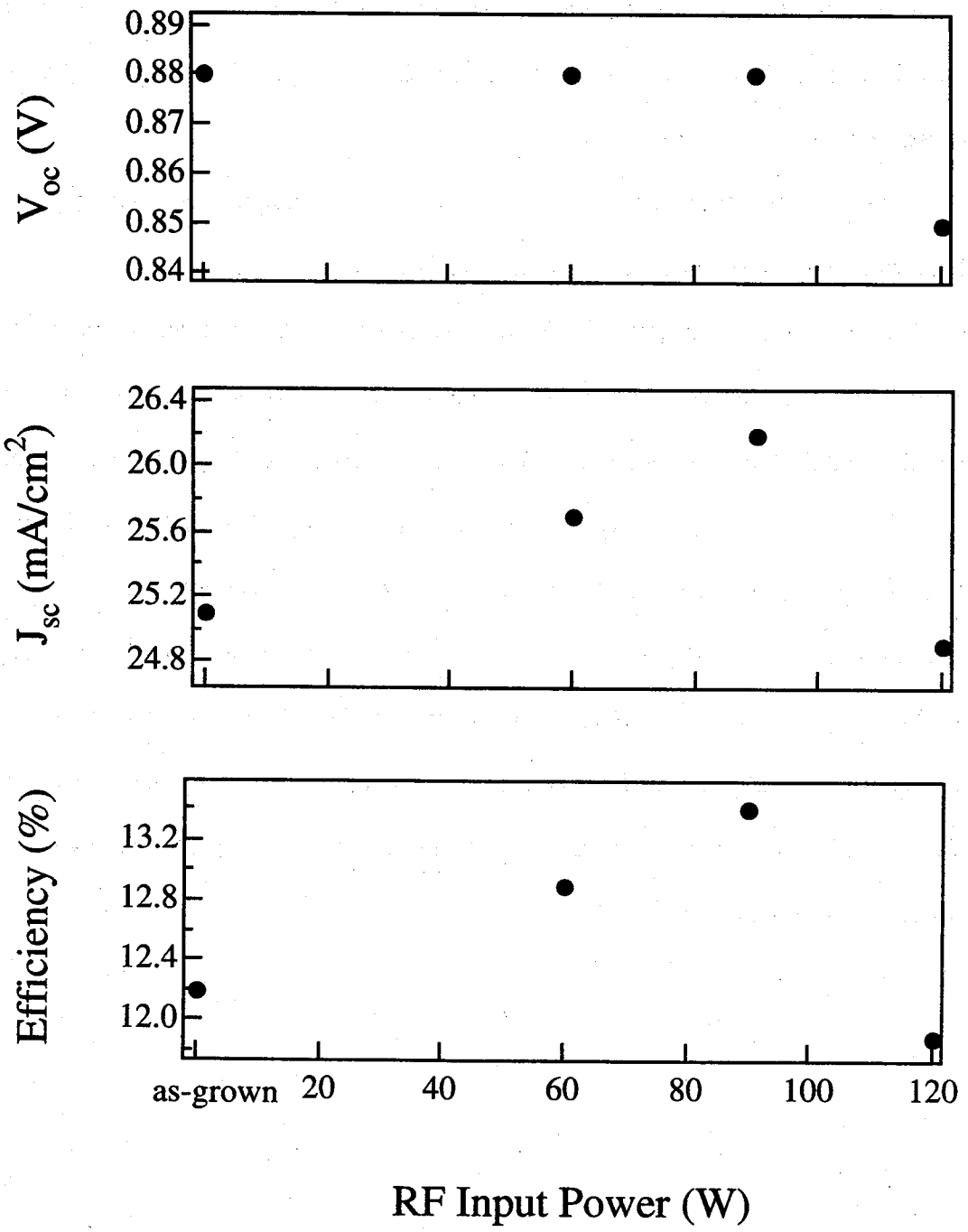

Fig. 3. 6 The photovoltaic properties of GaAs/Si solar cells as a function of RF plasma input power. The plasma exposure time is 60 min, and the temperature is 250°C. The post-passivation annealing conditions were fixed at 450°C for 10 min in AsH_3 ambient. The values were obtained from the without antireflection coating (ARC) cell.

cell became very leaky due to the plasma-induced damages. This means the AsH_3-annealing is very helpful to recover the plasma-induced damages. Both H_2 plasma passivation and AsH_3 post-passivation annealing play important roles in obtaining stable improved conversion efficiency of GaAs/Si solar cell. As the annealing temperature exceeds 650 °C, the photovoltaic properties of GaAs/Si solar cell were severely destroyed due to the activated plasma-induced damages, which is in good agreement with the lifetime results.

Figure 3.4 shows the quantum efficiency of the respective samples. The short wavelength quantum efficiency is improved by hydrogen plasma passivation.

In order to find the optimum condition for H_2 plasma exposure, the photovoltaic properties of GaAs/Si solar cells were measured as a function of the H_2 plasma exposure time and the plasma input power with a fixed annealing condition at 450°C for 10 min in AsH_3/H_2 ambient, which are shown in Fig. 3. 5 and 3. 6, respectively. For Fig. 3. 5, the RF input power was 90 W, and for Fig. 3. 6, the plasma exposure time was 60 min. It can be clearly seen that both the long exposure time and high plasma power negate the beneficial effects of H plasma passivation due to plasma-induced damages. Especially, the high RF plasma power (120 W) severely degraded the photovoltaic properties of the passivated GaAs/Si solar cell. It suggest that the high energetic ion caused the majority of the plasma-induced damages. In our case, the 90 W of plasma power and 1h exposure is the best conditions.

3. 4 Conclusion

In conclusion, H plasma passivation and annealing effects on photovoltaic properties of GaAs/Si solar cell are studied in detail. The minority carrier lifetime is increased due to the H passivation effects on defect-related nonradiative recombination centers. As a result, an effective increase of conversion efficiency of GaAs/Si solar cell is obtained. But the plasma-induced damages still restrict the practical application of H passivation technology on GaAs/Si solar cell. In order to further increase the conversion efficiency of the H_2 plasma passivated GaAs/Si solar cell, it needs to use some low damage plasam equipment, such as ECR plasma etc., to remove the negative effect of plasma-induced damages as best as possible.

References:

1)J. C. C. Fan, B. Y. Tsaur and B. J. Palm: *16th IEEE PVSEC Conf.* (San Diego, USA, 1982) p. 692.

2)M. Yamaguchi and C. Amano: J. Appl. Phys. **58** (1985) 3601.

3)T. Soga, M. Yang, T. Kato, T. Jimbo and M. Umeno: Mate. Sci. Forum **196-201** (1995) 1779.

4)K. Nozawa and Y. Horikoshi: Jpn. J. Appl. Phys. **31** (1991) L668.

5)M. Yang, T. Soga, T. Egawa, T. Jimbo and M. Umeno: Sol. Energy Mater. Sol. Cells **35** (1994) 45.

6)M. Yang, T. Soga, T. Jimbo and M. Umeno: Jpn. J. Appl. Phys. **33** (1994) 6605.

7)T. Soga, M. Yang, T. Jimbo and M. Umeno: Jpn. J. Appl. Phys. **35** (1995) 1401.

8)S. J. Pearton, W. C. Dautremont-Smith, J. Chevallier, C. W. Tu and K. D. Cummings: J. Appl. Phys. **59** (1986) 2821.

9)S. J. Pearton: J. Appl. Phys. **53** (1982) 4509.

10)E. K. Kim, H. Y. Cho, Y. Kim, H. S. Kim, M. S. Kim and S. K. Min: Appl. Phys. Lett. **58** (1991) 2405.

11)J. M. Zavada, S. J. Pearton, R. G. Wilson, C. S. Wu, M. Stavola, F. Ren, J, Lopata, W. C. Dautremont-Smith and S. W. Novak: J. Appl. Phys. **65** (1989) 347.

12)P. Friedel and S. Gourrier: Appl. Phys. Lett. **42** (1983) 509.

13)G. Wang, G. Y. Zhao, T. Soga, T. Jimbo and M. Umeno: Jpn. J. Appl. Phys. **37** (1998) L1280.

Chapter 4 Photoluminescence studies of hydrogen-passivated $Al_{0.13}Ga_{0.87}As$ grown on Si substrate by metalorganic chemical vapor deposition

4. 1 Introduction

III-V materials on Si substrates are useful for combining the superior electronic and optical properties of compound semiconductors with the matured technology of Si.[1] Among them, AlGaAs and AlGaAs/GaAs heterostructures grown on Si substrates are of great interest for the fabrication of, for example, high-performance lasers and tandem solar cells. Recently, a conversion efficiency of 21.4% was achieved for a AlGaAs/Si tandem solar cell.[2] However, compared to the most extensively investigated GaAs on Si epilayer, there have been few reports on the fundamental physical characteristics of the AlGaAs epilayer on Si. Photoluminescence (PL) is a nondestructive characterization technique used for the assessment of the optical quality of semiconductors. The incorporation of atomic hydrogen (H) into semiconductors not only can passivate the electrical activity of dangling or defective bonds,[3] but also help to clarify the origin of the luminescence.[4] In this chapter, we report the photoluminescence study of near-band-edge transitions and their hydrogen passivation effects on the $Al_{0.13}Ga_{0.87}As$ (3.0 μm) epilayer grown on a Si substrate. The organization of this chapter is as follows: In section 4. 2, the growth of AlGaAs layers on Si substrates are described. The AlGaAs epilayer and the change induced by H_2 plasma passivation on photoluminescence properties are characterized in chapter 4. 3. Finally, this chapter is summarized in section 4. 4.

4. 2 Experimental procedure

The epitaxial growth was performed by rf-heated atmospheric-pressure metalorganic chemical vapor deposition (MOCVD) on an n^+-Si substrate, oriented 2° off (100) toward [011], using the two-step growth technique. The source materials for Ga, Al and As were trimethylgallium (TMG), trimethylaluminum (TMA) and arsine (AsH_3), respectively. The heteroepitaxial growth sequence of $Al_{0.13}Ga_{0.87}As$ on a Si substrate was as follows. First, the Si substrate was etched in an aqueous solution of HF, and thermally heated at 1000°C for 10 min in a hydrogen ambient to remove the surface native oxide. Then, a 10-nm-thick GaAs low-temperature nucleation layer was grown at 400°C, upon which a 20-nm-thick GaAs buffer layer was grown at 750°C. Thereafter, a 3.0-μm-thick $Al_{0.18}Ga_{0.87}As$ layer was grown at 750°C. Lastly, a 10-nm-thick GaAs cap layer was grown to cover the underlying AlGaAs surface from air. All of the as-grown samples are n-type with a free-carrier concentration of 2×10^{17} cm^{-3} at room temperature due to Si autodoping from the substrate during the epitaxial growth process. After the growth, samples were cut into pieces and some of them were subjected to H_2 plasma exposure at 250°C for 1 h. Some of the passivated pieces were annealed at 450°C for 10 min in AsH_3/H_2 ambient to restore the free-carrier concentration. The H_2 plasma was excited by radio frequency (13.56 MHz) wave, at 0.1 Torr with an induced power of 90 W. After H_2 plasma exposure, the activity of the shallow donor (Si) was partly passivated and the carrier concentration was effectively reduced (1×10^{17} cm^{-3}), and the annealing completely restored the carrier concentration to its original value. This result is consistent with that of GaAs on Si.[5)]

For the PL measurements, the as-grown, the passivated, and the annealed samples were mounted in a cryostat which can be held at 4.2 K (liquid He), 77 K (liquid N_2) and room temperature (RT). A 514.5 nm Ar-ion laser was used as an excitation source, and its power was increased from 5 mW to 500 mW to study the dependence of PL intensity and peak energy on excitation intensity. The luminescence was analyzed using a spectrometer and detected by a

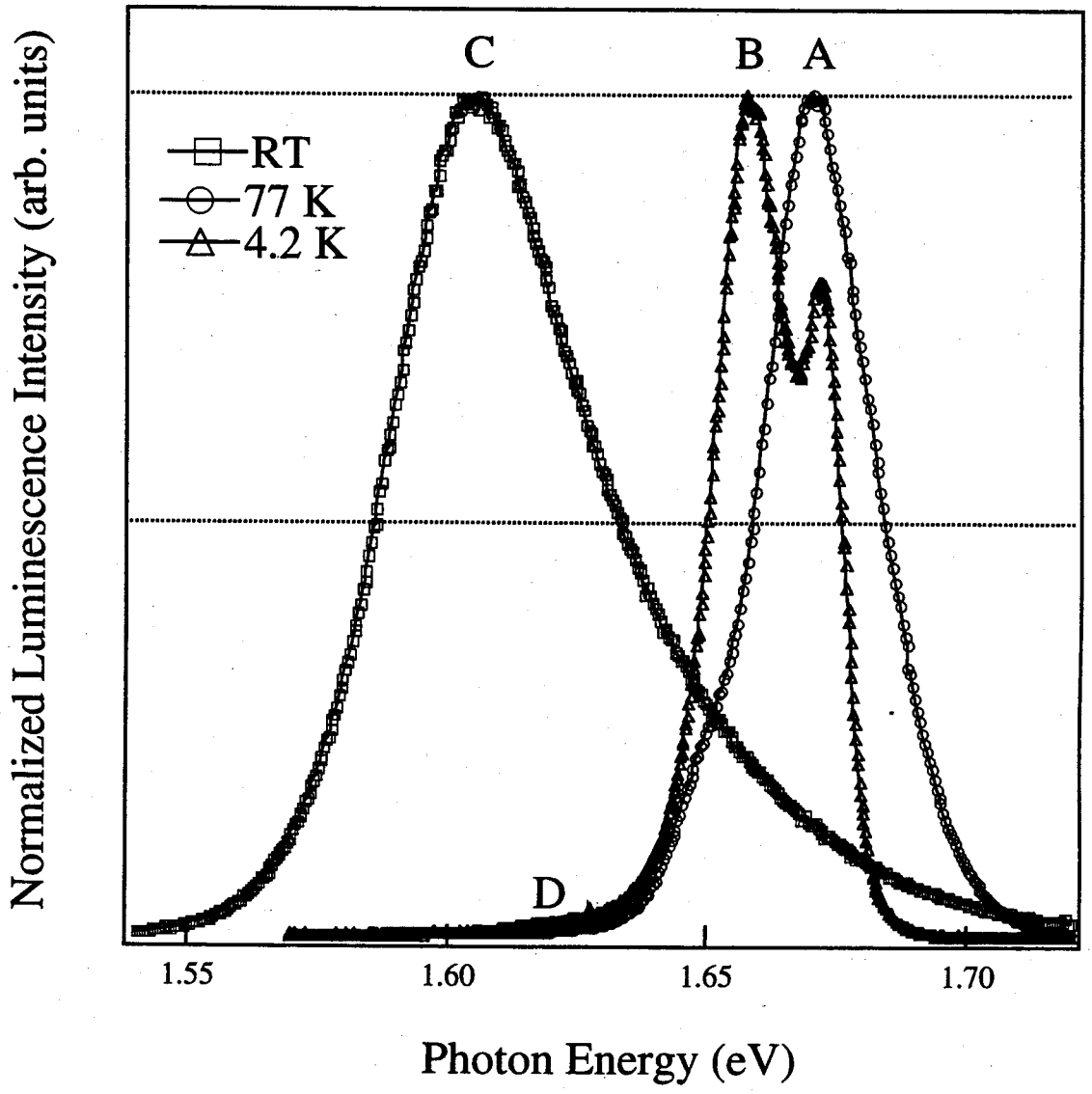

Fig. 4. 1. Normalized PL spectra of as-grown $Al_{0.13}Ga_{0.87}As$ on Si measured for three temperatures, 4.2 K, 77 K and room temperature (RT), using a power density of about 15.1 W/cm^2. The split width of the spectrometer was 200 μm at 4.2 K, 1 mm at 77 K and 3 mm at room temperature (RT).

photomultiplier tube (PMT) with a GaAs photocathode connected to a lock-in amplifier.

4. 3 Characterization of the photoluminescence properties for AlGaAs on Si

Figure 4. 1 shows the measured PL spectra of the unintentionally doped $Al_{0.13}Ga_{0.87}As$ grown on the Si substrate before H plasma passivation. At 4.2 K, an intense peak B at 1.658 eV, a relatively low-intensity peak A at 1.672 eV, and a faint emission tail peak D towards the low-energy end can be observed. At 77 K, the PL spectrum is dominated by peak A, while peak B appears only as a weak shoulder. As the temperature increases to room temperature, a single broad spectral feature, peak C, can be observed at 1.605 eV. We identify the room-temperature peak C as a conduction-band-to-valence-band transition, since the exciton- and shallow-donor-related luminescence is thermally quenched at room temperature and the band-to-band (BB) recombination will dominate the spectrum.[6)]

In order to investigate the origin of peaks A and B, the dependence of PL intensity (I) on excitation intensity (J) was measured at 4.2 K. Figure 4. 2 shows the PL intensities of peaks A and B of the as-grown $Al_{0.13}Ga_{0.87}As$ on Si sample as a function of J. The intensity dependence of the near-band-gap luminescence lines can be described in general by a power law $I = J^k$ where J is varied over a range of less than two orders of magnitude.[7)] As shown in Fig. 2(a), both emission peaks show a similar sublinear power-law dependence ($k<1$). A theoretical work by Schmidt et al. indicates that the sublinear dependence occurs for free-to-bound ($e - A^o$) and donor-acceptor pair ($D^o - A^o$) recombination, but that superlinear dependence occurs for both free- and bound-exciton recombination.[7)] Therefore, both peaks A and B can be assigned to free-to-bound or donor-acceptor recombination. However, as shown in Fig.4. 2(b), as the excitation intensity increases from 0.47 W/cm^2 to 60.3 W/cm^2, peak B exhibits a 2 meV shift toward higher energies, whereas peak A exhibits almost no shift (<1 meV). This suggests that peak B is results from a donor to acceptor transition, since M. I. Nathan et al found that in closely compensated GaAs the

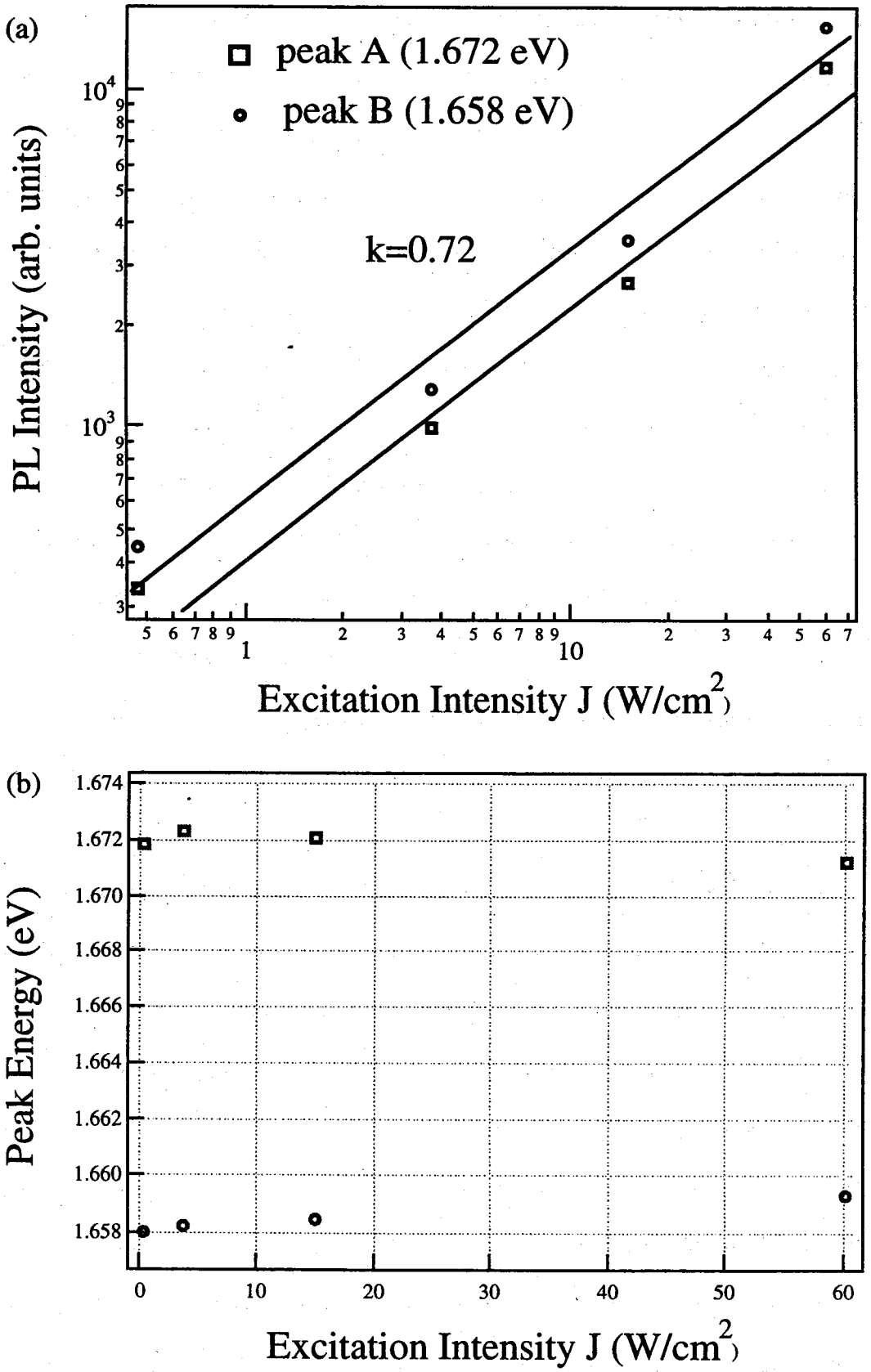

Fig. 4. 2. Dependence of (a) PL intensity and (b) peak energy on the excitation intensity J for peak A (1.672 eV) and peak B (1.658 eV) of as-grown $Al_{0.13}Ga_{0.87}As$-on-Si, measured at 4.2 K.

emission spectrum shifts to higher energies as the excitation rate increases. Considering the high level of Si autodoping, we assign peak A to a free-to-bound (e - A^o) and peak B to donor Si - acceptor pair (D^o_{si} - A^o) transitions. As the shift is very margin, it needs other evidence to prove above assignment of peaks A and B. This assignment is confirmed by temperature characteristics described above. As the temperature increases from 4.2 K to 77 K, Si becomes ionized and the e - A^o transition peak A dominates the PL spectrum (Fig. 1). Using the band-gap value obtained from the room-temperature PL measurement, we deduce that the 4.2 K band edge E_g of $Al_{0.13}Ga_{0.87}As$ on Si should be sited at 1.705 eV, according to Varshni's semi-empirical relation.[8] We can see that the free-to-bound transition peak A is lower than E_g by nearly 33 meV, which is close to the carbon (A^o_c) acceptor activation energy (28 meV) in $Al_{0.13}Ga_{0.87}As$.[6] The temperature-induced change of the tensile strain caused by the mismatch of the thermal expansion coefficients between $Al_{0.13}Ga_{0.87}As$ and the Si substrate was not considered in the above calculation, which will increase with a decrease in temperature and further reduce the energy band gap.[1] Since carbon is a well-known residual impurity in MOCVD-grown AlGaAs and GaAs, we assume that the neutral acceptor A^o in our sample is carbon (A_c^o).[9]

Figure 4. 3 shows the 4.2 K semilog PL spectra of H_2 plasma passivated, annealed and as-grown samples. Due to the large overlap of peaks A and B, we separated them using a Gaussian distribution function to determine the exact peak energies; the fitted results are given in Table 4. 1. Compared to those of as-grown samples, the PL spectra of H_2 plasma passivated and annealed samples show some noteworthy features.

(i) After H_2 plasma passivation, the intensity of peak B (D^o_{si} - A^o_c) is enhanced as much as 1.5 times, whereas the intensity of peak A (e - A^o_c) is dramatically decreased (0.42 times). As a result, the integrated intensity of the 4.2 K PL spectrum of the H plasma passivated sample shows some increase compared to that of the as-grown one. Furthermore, the emission energy of peak B for the H_2 plasma passivated sample shows a redshift of nearly 2 meV towards the low-energy edge compared to that of the as-grown sample. In contrast, little shift of peak A is observed after H_2

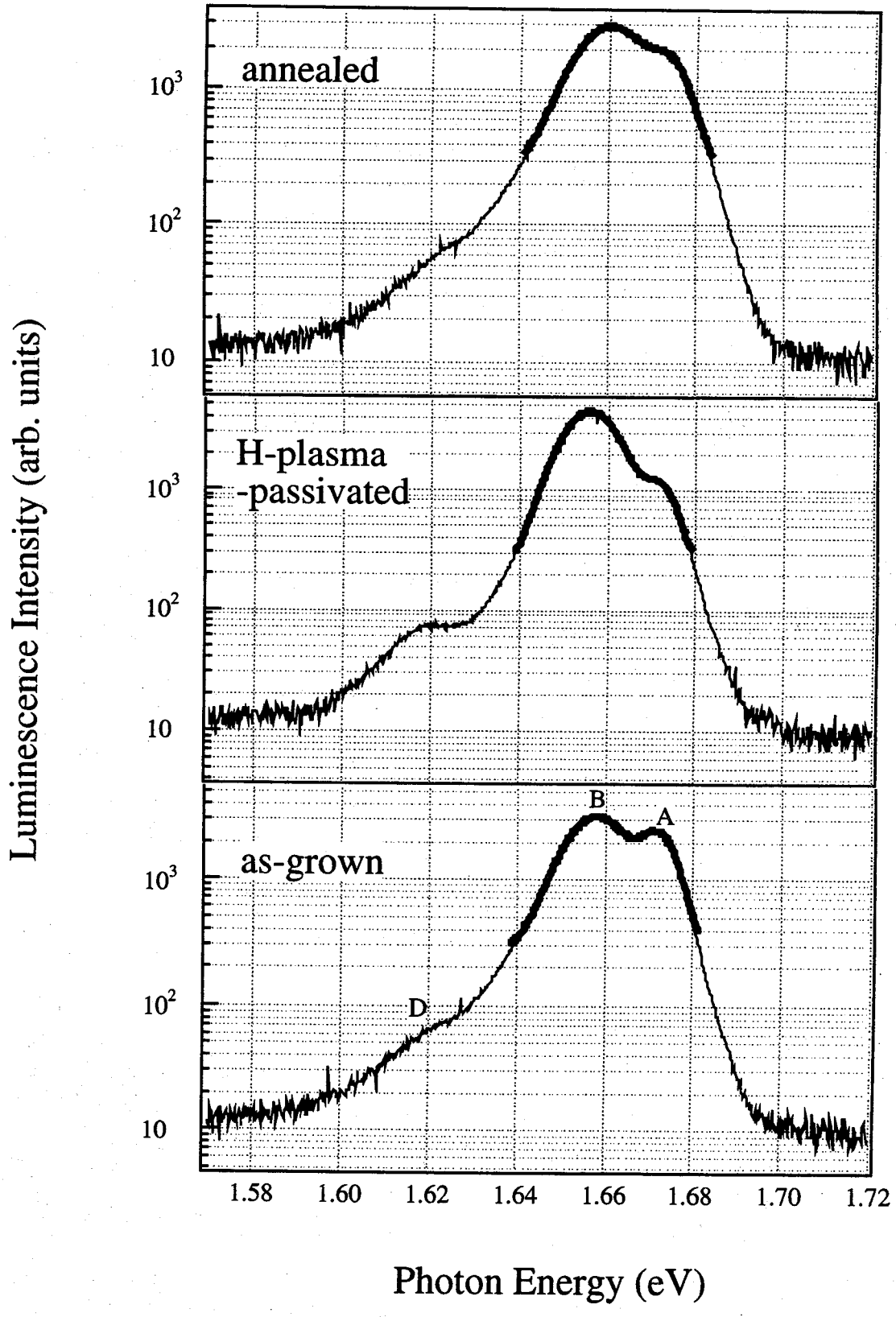

Fig. 4. 3. PL spectra for as-grown, H-plasma-passivated and annealed passivated samples on a semilogarithmic scale, measured at 4.2 K using a power density of about 15.1 W/cm^2. The dotted lines indicate the fitted results.

Table 4. 1 The 4.2 K PL spectra fitting results of emission energy (E), PL peak intensity (I) and full-width at half maximum (FWHM).

Sample number	$(E)_A$ (eV)	$(I)_A$ (a.u.)	$(FWHM)_A$ (meV)	$(E)_B$ (eV)	$(I)_B$ (a.u.)	$(FWHM)_B$ (meV)
as-grown	1.6724	1889	5.3	1.6582	2908	9.3
H_2 plasma passivated	1.6721	785	5.0	1.6563	4223	8.8
annealed	1.6742	1062	5.7	1.6605	2639	10.4

plasma passivation.

(ii) The lowest energy peak D (~1.619 eV) can be more clearly resolved after H_2 plasma passivation due to an increase of intensity. The peak energy is about 38 meV lower than the nearest high-energy peak, indicating that this emission is a GaAs-like longitudinal optical (LO) phonon replica of the D_{si}° - A_c° transition.[10)]

(iii) After annealing at 450°C for 10 min, the intensities of peaks B and D are reduced almost to their original values. However, the intensity of the free electron to carbon acceptor transition of the annealed passivated sample is still weak (~50%) compared to that of the as-grown sample .

Some conclusions can be drawn from the distinct features of peaks A and B in the PL spectra of H_2 plasma passivated and as-grown samples. First, the reduction of the emission intensity of electron to acceptor (e - A°) transition peak A suggests that the electrically active residual impurity carbon (C) in $Al_{0.13}Ga_{0.87}As$ on Si can be effectively passivated by H_2 plasma exposure, since the rate of the electron to acceptor (e - A°) transition is determined by the acceptor concentration N_A. This conclusion is consistent with the fact that hydrogenation can passivate the carbon (C) in AlGaAs grown on GaAs substrate.[11)] The theoretical interpretation of the passivation mechanism of carbon (C) by H is that the valence electron of the atomic H can recombine with a free hole, leaving a proton (H^+) and a negatively charged C acceptor which form a pair due to Coulombic attraction, resulting in the electrical deactivation of C.[12)] Second, the redshift of the donor-acceptor pair (D° - A°) transition following H_2 plasma passivation suggests that H incorporation increases the nearer donor-acceptor pair separation and weakens the Coulomb interaction between them, and thus decreases the emission energy.[13)] This indicates that H passivation effectively decreases the total impurity concentration. Although the donor-acceptor pair (D° - A°) transition is in proportion to the amount of electrically active donor and acceptor concentrations, the PL intensity of peak B is still enhanced. Considering the improvement in the 4.2K PL integrated intensity for the H_2 plasma passivated samples, this enhancement can be attributed to the passivation of nonradiative recombination channels. This interpretation is also strongly supported by the results obtained from

our deep-level transient spectra (DLTS) measurement which exhibited a decrease in the integrated concentration of deep levels in $Al_{0.13}Ga_{0.87}As$ on Si following the H plasma passivation. Third, the incomplete recovery of the intensity of the free-electron-to-carbon transition (D_{si}° - A_c°) of the annealed sample suggests that the passivaton effect of residual impurity carbon remains even after the free-electron concentration is restored by 450°C annealing. This indicates that some parts of the H-related species are stable after the 450°C annealing treatment. On the other hand, the small decrease in the PL efficiency of the annealed sample compared to that of the as-grown one may be due to some plasma-induced damages which quench the PL intensity.[14)]

4. 4 Conclusion

In summary, we have investigated the H_2 plasma passivation effect of MOCVD-grown $Al_{0.13}Ga_{0.87}As$ on Si, using PL spectroscopy. It has been found that the 4.2 K PL intensity increases for the H_2 plasma passivated sample, owing to the passivation of nonradiative recombination centers. The passivation of residual impurity carbon in the $Al_{0.13}Ga_{0.87}As$ on Si epilayer was directly confirmed based on the observations of the 4.2 K PL spectra of the samples. The passivation effect is found to persist even following annealing at 450°C for 10 min. This result creates renewed prospects for the application of AlGaAs on Si to practical devices.

References:

1) S. F. Fang, K. Adomi, S. Lyer, H. Morkoc, H. Zabel, C. Choi and N. Otsuka: J. Appl. Phys. **68** (1990) R31.

2) T. Soga, K. Baskar, T. Kato, T. Jimbo and M. Umeno: J. Cryst. Growth **174** (1997) 579.

3) S. J. Pearton, J. W. Corbett and M. Stavola: *Hydrogen in Crystalline Semiconductors* (Springer, Berlin, 1992).

4) A. Bosacchi, S. Franchi, E. Gombia, R. Mosca, A. Bignazzi, E. Grilli, M. Guzzi and R. Zamboni: Jpn. J. Appl. Phys. **33** (1994) 3348.

5) J. Chevallier, W. C. Dautremont-Smith, C. W. Tu and S. J. Pearton: Appl. Phys. Lett. **49** (1985) 406.

6) L. Pavesi and M. Guzzi: J. Appl. Phys. **74** (1994) 4779.

7) T. Schmidt, K. Lischka and W. Zulehner: Phys. Rev. B **45** (1992) 8989.

8) Y. P. Varshni: Physica **34** (1967) 149.

9) Y. Chen, A. Freundlich, H. Kamada and G. Neu: Appl. Phys. Lett. **54** (1989) 45.

10) V. Reide, H. Sobotta, H. Neumann, I. Gregova, S. Kamba and V. Vorlizek: Cryst. Res. Technol. **24** (1989) 909.

11) M. Proctor, G. Oelgart, G. Lippold and F. K. Reinhart: Appl. Phys. Lett. **62** (1993) 846.

12) N. Pan, S. S. Bose, M. H. Kim, G. E. Stillman, F. Chambers, G. Devane, C. R. Ito and M. Feng: Appl. Phys. Lett. **51** (1987) 596.

13) J. I. Pankove: *Optical Processes in Semiconductors* (Prentice-Hall Inc., Englewood Cliffs, New Jersey, 1975).

14) V. Swaminathan, U. K. Chakrabarti, W. S. Hobson, R. Caruso, J. Lopata, S. J. Pearton and H. S. Luftman: J. Appl. Phys. **68** (1990) 902.